nature communications

Article

https://doi.org/10.1038/s41467-024-54661-9

Camrelizumab plus apatinib for previously treated advanced adrenocortical carcinoma: a single-arm phase 2 trial

Received: 3 April 2024

Accepted: 16 November 2024

Published online: 29 November 2024

Check for updates

Yu-Chun Zhu[1,4], Zhi-Gong Wei[2,4], Jing-Jing Wang[2], Yi-Yan Pei[2], Jing Jin[2], Dong Li[3], Zhi-Hui Li[3], Zhe-Ran Liu[2], Yu Min[2], Rui-Dan Li[2], Li Yang[2], Ji-Yan Liu[2], Qiang Wei[1] & Xing-Chen Peng[2]

Adrenocortical carcinoma (ACC) is a rare, aggressive malignancy with a poor prognosis. Therapeutic options for patients with advanced ACC who have failed standard treatments are limited. Single-agent immunotherapy as a second-line treatment has shown unsatisfactory clinical outcomes. This phase II trial (NCT04318730) evaluated the efficacy and safety of the PD-1 inhibitor camrelizumab combined with the VEGFR inhibitor apatinib in previously treated advanced ACC. The primary endpoint was objective response rate (ORR). The secondary endpoints included progression-free survival (PFS), overall survival (OS), and safety. A total of 21 patients with advanced ACC received at least one dose of camrelizumab and apatinib. The ORR was 52% (95% CI, 30–74%), meeting the primary endpoint, and the disease control rate (DCR) was 95% (95% CI, 76–100%). The median PFS was 13.3 months (95% CI, 8.4–NE), and the median OS was 20.9 months (95% CI, 11.0–NE). The most common grade 3–4 treatment-related adverse events were alanine aminotransferase elevation, aspartate aminotransferase elevation, and lymphopenia. Predefined exploratory analyses indicated that patients with higher peripheral blood CXCR3 + CD8 + T cell abundance, lower immunosuppressive CD4 + T cell abundance, and higher overlap of clonotypes between tumor-infiltrating T cells and circulating T cells, were more likely to respond favorably to the combined therapy.

Adrenocortical carcinoma (ACC) is a rare, aggressive malignancy with a poor prognosis and limited treatment options, resulting in a 5-year survival of only 13% for stage IV disease[1,2]. Mitotane, a synthetic derivative of the pesticide dichlorodiphenyltrichloroethane, is the only approved drug for ACC. It exhibits adrenolytic activity but has limited efficacy, and is associated with serious toxicity[3,4]. Cytotoxic chemotherapy remains a cornerstone in the treatment of advanced ACC. The combination of etoposide, doxorubicin, and cisplatin (EDP) with mitotane is currently the standard first-line therapy based on the results of the FIRM-ACT study. However, the response rate is only 23% and median duration of progression-free survival (PFS) is only 5.0 months[5]. For patients with advanced ACC whose disease progresses after Mitotane and/or chemotherapy, therapeutic options are severely limited.

Immune checkpoint inhibitors (ICIs), such as monoclonal antibodies targeting programmed cell death-1 (PD-1) or its ligand (PD-L1), have shown promise in the treatment of ACC[6–9]. However, the efficacy of anti-PD-1/PD-L1 monotherapy for advanced ACC remains

[1]Department of Urology, West China Hospital, Sichuan University, Chengdu, China. [2]Department of Biotherapy, Cancer Center and State Key Laboratory of Biotherapy, West China Hospital, Sichuan University, Chengdu, China. [3]Department of Oncology, The General Hospital of Western Theater Command, Chengdu, China. [4]These authors contributed equally: Yu-Chun Zhu, Zhi-Gong Wei. e-mail: pxx2014@163.com

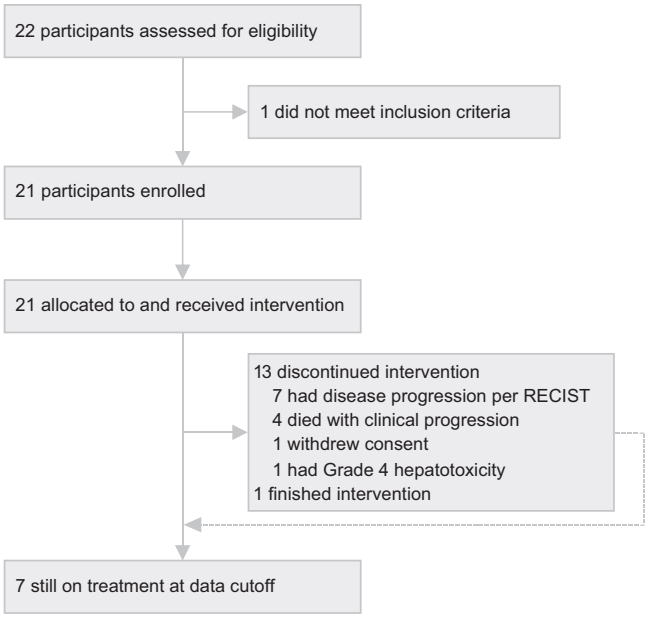

Fig. 1 | Trial profile. A total of 22 patients were assessed for eligibility in this trial. After excluding one patient who did not meet the inclusion criteria, 21 patients received at least one dose of camrelizumab plus apatinib. As of the data cutoff, seven patients remained on treatment.

unsatisfactory, with response rates ranging from 10% to 23%[7,10,11]. The potential for immunoresistance in ACC patients, due to both tumor-secreted endogenous glucocorticoids and glucocorticoid supplementation in those treated with mitotane, may reduce the effectiveness of single-agent immunotherapy[12]. Therefore, combining immune checkpoint inhibitors (ICIs) with other drugs might be more effective than immunotherapy alone.

Vascular endothelial growth factor (VEGF) and its receptor (VEGFR) are highly expressed in ACC[13]. A phase II study demonstrated that anti-angiogenic therapy targeting VEGF/VEGFR has modest anti-tumor activity in patients with ACC[14]. Anti-angiogenesis therapy has been found to reprogram the tumor immune microenvironment in preclinical studies[15]. Recent clinical studies have also confirmed the synergistic anti-tumor effects of combining ICIs with anti-angiogenesis therapy in various advanced tumors[16–20]. Additionally, a retrospective case series reported that pembrolizumab, a PD-1 inhibitor, combined with lenvatinib, a multikinase inhibitor targeting VEGFR, achieved promising objective responses with manageable toxicity in ACC patients who had previously progressed through several lines of therapy[21].

Here, we show that the combination of the PD-1 inhibitor camrelizumab and the VEGFR2-targeted small molecular tyrosine kinase inhibitor (TKI) apatinib has promising activity and an acceptable safety profile in patients with previously treated advanced ACC. Moreover, we have explored relevant molecular biomarkers that may be associated with the clinical efficacy of the camrelizumab-apatinib combination therapy.

Results

Patients

Between November 2020 and April 2023, a total of 22 patients were assessed for eligibility. Of these, 21 patients received at least one dose of camrelizumab plus apatinib and were included in the modified intention-to-treat (mITT) population (Fig. 1). Among the 21 patients, eight (38%) had hormonally functioning tumors, with six producing cortisol and two producing both cortisol and androgens. All patients had previously received at least one type of anticancer therapy, with 90% (19/21) having received mitotane and 57% (12/21) having received chemotherapy (Table 1).

As of the data cutoff (December 1, 2023), seven patients were still undergoing treatment. One patient completed the two-year study intervention and achieved a durable response lasting 33 months. Thirteen patients discontinued treatment, seven due to radiographic disease progression, four due to death related to clinical progression, one due to withdrawal of consent after receiving 12 cycles of study drugs, and one due to grade 4 hepatotoxicity, leading to permanent discontinuation of all study drugs.

Anti-tumor activity

Of the 21 patients who received the treatment, 11 (52%; 95% confidence interval [CI], 30–74%) achieved objective responses, meeting the primary endpoint. All these responses were partial responses (PRs), with no complete responses (CRs) observed. Nine additional patients (43%) exhibited stable disease (SD), and one patient (5%) had progressive disease (PD) as the best response at the end of follow-up (Fig. 2 and Supplementary Fig. 1). The disease control rate (DCR), defined as the proportion of patients achieving CR, PR, or SD, was 95% (95% CI, 76–100%). For the 11 patients who achieved PR, the median time to response was 2.8 months (range, 0.8–12.6), and median duration of response was not reached (Table 2).

For patients with non-hormonally functioning tumors, 69.2% (9/13) achieved PRs compared to 25% (2/8) for those with hormonally functioning tumors ($p = 0.08$). Responses were observed across various subgroups, irrespective of age, sex, Eastern Cooperative Oncology Group (ECOG) performance status, liver metastasis, lung metastasis, number of metastatic sites, prior chemotherapy, and prior mitotane treatment (Supplementary Fig. 2).

Survival outcomes were also included as secondary endpoints. After a median follow-up duration of 17.5 months (range, 2.1–37.1 months) for all patients in the mITT set, nine deaths were reported, all of which were cancer-specific. Among these patients, two had achieved a PR, six had SD, and one had PD as the best response. Notably, eight (72.3%) of the 11 patients who achieved PR were still alive without disease progression by the cutoff date (Fig. 3A). The median PFS was 13.3 months (95% CI, 8.4–NE) and the median overall survival (OS) was 20.9 months (95% CI, 11.0–NE). The 1-year PFS rate was 57.1%, and 1-year OS rate was 74.5% (Fig. 3B, C).

Safety

Treatment-related adverse events (TRAEs), as a secondary endpoint, were assessed in 21 patients, with grade 3–4 TRAEs occurring in nine patients (Table 3). The most common grade 3–4 TRAEs were alanine aminotransferase elevation, aspartate aminotransferase elevation, and lymphopenia. No grade 5 TRAEs leading to death were reported. The response rate among patients who experienced grade 3–4 TRAEs was 66.7% (6/9), compared to 41.7% (5/12) in those who did not; however, this difference was not statistically significant ($p = 0.387$). Univariate Cox regression analysis showed no significant difference in the risk of death between patients who experienced grade 3–4 TRAEs and those who did not (HR 0.72, 95% CI 0.19–2.70; $p = 0.62$). Only one patient permanently discontinued all study drugs after receiving one treatment cycle because of severe hepatotoxicity. Despite this, the patient achieved a PR as the best response, and the disease has remained controlled off therapy for more than eight months without additional anti-tumor treatment. Moreover, nine patients experienced temporary discontinuation of camrelizumab and dose reduction of apatinib due to TRAEs. The administration of camrelizumab was delayed in seven patients due to COVID-19-related factors.

Exploratory analyses

Tumor immune microenvironment. Pretreatment archival tumor tissue samples were collected from 14 primary lesions and 2 recurrent/

https://doi.org/10.1038/s41467-024-54661-9

Table 1 | Baseline characteristics

Characteristic	Patients (*N* = 21)	
Age, years	48	(35.5–55)
>50	9	(43%)
≤50	12	(57%)
Sex		
Female	13	(62%)
Male	8	(38%)
ECOG performance status		
0	14	(67%)
1	7	(33%)
Smoking history		
Never	18	(86%)
Current	2	(10%)
Former	1	(5%)
BMI, kg/m^2	22	(21–25)
≥24	8	(38%)
<24	13	(62%)
Site of metastases		
Lung	14	(67%)
Liver	8	(38%)
Tumor bed	7	(33%)
Others*	10	(48%)
Prior regional therapy		
Adrenalectomy	21	(100%)
Radiotherapy	3	(14%)
Prior systemic therapy		
Platinum-based therapy	12	(57%)
Mitotane	19	(90%)
Hormonally functioning tumor		
Yes	8	(38%)
Cortisol	6	(28.6%)
Cortisol and androgens	2	(9.5%)
No	13	(62%)
Tumor mutation burden†	1.9	(0–4.5)
≥10	2	(10%)
<10	18	(86%)
Not evaluable	1	(5%)
PD-L1 combined positive score		
≥1	2	(10%)
<1	18	(86%)
Not evaluable	1	(5%)
MSI status†		
MSI-H	2	(10%)
MSS	18	(86%)
Not evaluable	1	(5%)

Data are n (%) or median (IQR), unless otherwise stated. Overall percentages might not add up to 100% due to rounding. *Others included abdominal and retroperitoneal lymph nodes, bone, and muscle. †Two participants were evaluated based on peripheral blood.
ECOG Eastern Cooperative Oncology Group, *MSI* microsatellite instability, *MSS* microsatellite stability.

metastatic lesions to evaluate the tumor immune microenvironment. The expression levels of CD4 and CD8 were consistently low, with most samples exhibiting less than 5% CD4+ or CD8+ cells (Fig. 4A). Treatment response was not significantly associated with the percentages of CD4 + , CD8 + , or CD56+ cells (Fig. 4B and Supplementary Fig. 3). Moreover, there was no significant difference in the percentages of CD4 + , CD8 + , or CD56+ cells between hormonally functioning and non-hormonally functioning tumors (Supplementary Fig. 4).

T-cell receptor (TCR) repertoires. The level of TCR diversity in peripheral blood T cells and the clonality of tumor-infiltrating T cells did not differ significantly between responders and nonresponders (Fig. 4C). However, correlation analysis revealed a significant correlation between TCR diversity and the best tumor size reduction (r = 0.49, $p = 0.02$) (Supplementary Fig. 5). Responders also had a significantly higher overlap index (OLI) compared to nonresponders ($p = 0.04$) (Fig. 4C).

Systemic immunity. Flow cytometry analyses of pretreatment peripheral blood showed that patients with a higher baseline percentage of CD8 + T cells were more likely to respond to combined therapy ($p = 0.002$), while a trend towards a higher percentage of CD4 + T cells was observed in nonresponders ($p = 0.055$). The baseline CD4 + /CD8 + T cell ratio was significantly lower in responders ($p = 0.002$) (Fig. 4D). After two treatment cycles, nonresponders showed a tendency for a decline in CD4 + T cells (Supplementary Fig. 6), which was accompanied by a significant decrease in the CD4 + / CD8+ T cell ratio ($p = 0.009$) (Fig. 4E). CyTOF analysis was further used to investigate the impact of systemic immune response on treatment outcomes. Similar trends were observed in the baseline abundance of CD4+ and CD8 + T cells, although these differences did not reach statistical significance (Supplementary Fig. 7). More specifically, responders showed increased expression of the chemokine receptor CXCR3 in CD8 + T cells, particularly in naïve CD8 + T cells ($p = 0.017$) (Fig. 4F, G). CXCR3 is known for its role in regulating the migration, differentiation, and activation of immune cells. Additionally, the expression of TIM-3, an immunosuppressive molecular, was significantly decreased in CD4 + T cells from patients who responded to treatment ($p = 0.03$) (Supplementary Fig. 8).

PD-L1 and MSI status. The level of PD-L1 expression was determined using the combined positive score (CPS). Only two patients (10%) were PD-L1 positive with a CPS ≥ 1; one patient had SD as the best response (CPS = 2), while the other achieved a PR (CPS = 5). The patient with PR also had both a high tumor mutational burden (TMB) and microsatellite instability-high (MSI-H) status. Notably, only two patients had MSI-H tumors.

Genetic alterations and gut microbial diversity. Next-generation sequencing (NGS) results are detailed in Fig. 5A and Supplementary Fig. 9. The most frequently mutated genes were *CKD4* (38.1%), *KRAS* (33.3%), *PDGFRA* (33.3%), *KDR* (28.6%), *KIT* (28.6%), and *MDM2* (28.6%). No specific somatic alterations were associated with treatment response (Supplementary Table 1). We also analyzed the gut microbiota composition and diversity from fecal samples collected prior to treatment (7 from responders and 4 from nonresponders). Microbiota α diversity, measured by the Shannon index and Ace index at the OTU level, was similar between responders and nonresponders (Fig. 5B). Moreover, β diversity analysis assessed by PCoA revealed no significant association between gut microbiota composition and treatment response (Fig. 5C).

Discussion

This prospective study demonstrated that the combination of anti-PD-1 and anti-VEGFR therapy provides promising clinical activity with an acceptable safety profile in advanced ACC patients who have progressed after standard therapy. As a second-line therapy, the combination of camrelizumab and apatinib achieved an objective response rate (ORR) of 52% and a durable survival benefit, which is higher than the published data for pembrolizumab (a PD-1 inhibitor) monotherapy

https://doi.org/10.1038/s41467-024-54661-9

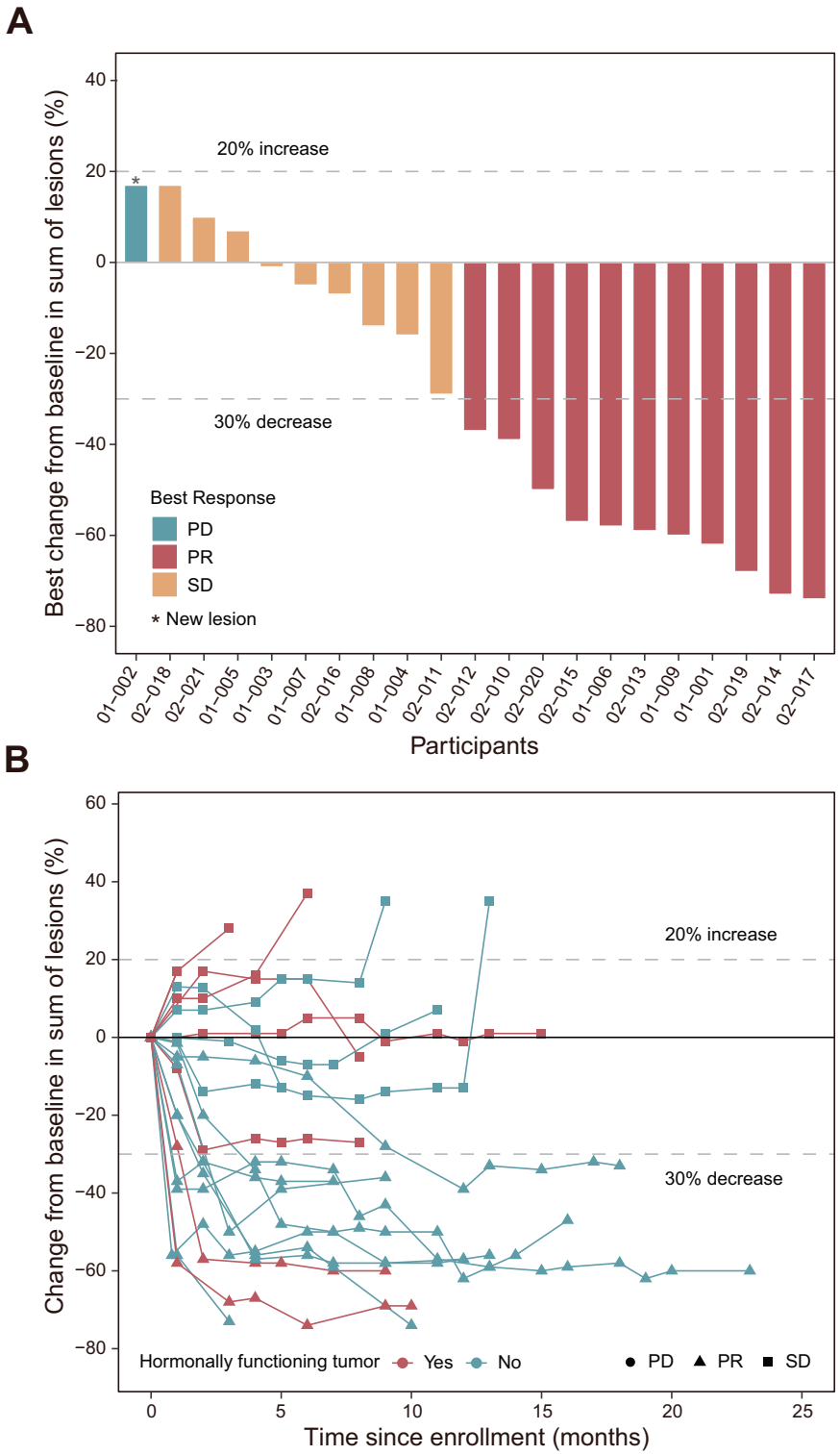

Fig. 2 | Tumor responses in individual patients. A Best change from baseline in the sum of the tumor size. Each bar represents one patient ($n = 21$). **B** Percentage change from baseline in target lesions over time ($n = 21$). Each curve represents one patient. PD progressive disease, PR partial response, SD stable disease. Source data are provided as a Source Data file.

(14–23%)[7,11] and exceeds the response rates with EDP plus mitotane in the first-line setting (23%)[5]. Moreover, this study reported that higher peripheral blood CXCR3 + CD8 + T cell abundance, lower immunosuppressive CD4 + T cell abundance, and higher overlap of clonotypes between tumor-infiltrating T cells and circulating T cells were potentially associated with a more favorable response to camrelizumab plus apatinib therapy.

Simultaneous inhibition of the VEGF-VEGFR2 and PD-1-PD-L1 pathways results in a synergistic anti-tumor effect by promoting tumor vascular normalization and enhancing immune cell infiltration[22]. Apatinib, a small molecule inhibitor of VEGFR-2, combined with the PD-1 inhibitor camrelizumab, has demonstrated superior efficacy across several malignancies in clinical trials[17,20,23,24], but there have been no reported experiences in patients with ACC to date. Our prospective study shows

the promising activity of camrelizumab plus apatinib as a second-line or later therapy for this rare and aggressive disease, with a manageable toxicity profile. In our study, all participants had progressed on at least one prior treatment. To date, only two of the eleven responding patients have died, indicating a sustained survival benefit. Our findings suggested that this combined regimen could serve as an alternative salvage therapy following the failure of standard therapy. Additionally, patients with non-hormonally functioning tumors may be more likely to benefit from camrelizumab plus apatinib. Overcoming potential inherent resistance to immunotherapy due to excess glucocorticoid production by the tumors remains a challenge for the treatment of ACC[25].

The observed safety profile of camrelizumab plus apatinib was consistent with the known individual toxicities of each drug, as well as with findings from previous studies[19,20,26]. The most commonly reported grade 3–4 adverse events were related to hepatotoxicity, and no treatment-related deaths occurred. The incidence of grade 3–4 adverse events was lower in patients receiving this combination compared to those treated with mitotane plus chemotherapy (43% vs. 58%)[5]. Only one patient permanently discontinued treatment due to uncontrollable transaminase elevation. Notably, this patient achieved a PR despite receiving only one cycle of camrelizumab, with remission lasting more than eight months. Previous studies have suggested that adverse events are more likely to occur in patients who respond to ICI treatment, both in ACC[7,9] and other cancers[27]. However, our study did not find evidence that TRAEs were associated with a favorable response or improved clinical outcomes.

Table 2 | Treatment response and outcomes

	Patients (*N* = 21)	
Complete response	0	
Partial response	11	(52%)
Stable disease	9	(43%)
Progressive disease	1	(5%)
Objective response rate	52%	(30%–74%)
Disease control rate	95%	(76%–100%)
Median duration of response, months		Not reached
Median progression-free survival, months	13.3	(95% CI: 8.4–NE)
Median overall survival, months	20.9	(95% CI: 11.0–NE)

Data are n (%) or % (95% CI), unless otherwise stated. All objective responses in this study were classified as partial responses by RECIST v1.1.

Our exploratory analyses aimed to identify potential response-related biomarkers for camrelizumab plus apatinib in ACC from multiple perspectives. Due to variations in cutoff values, reported rates of positive PD-L1 expression in ACC range from 10.7% to 29% (10.7%[28]; 21%[7]; 29%[6]), compared to 10% in our study, as determined by CPS. With only two patients testing positive for PD-L1, we were unable to analyze the correlation between PD-L1 expression and treatment efficacy. A similar limitation applies to MSI/MMR analysis. Importantly, the majority of patients who lacked positive tumor PD-L1 expression or MSI-H status still responded well to the combination therapy of camrelizumab and apatinib. This suggests that the relationship between these biomarkers and treatment response in ACC requires further investigation in the context of combined therapy.

The efficacy of immunotherapy in cancer patients has been linked to the immune composition within the tumor microenvironment[29], as well as the immune landscape in the blood circulation system[30]. We analyzed pre-treatment tumor tissues to assess the immune microenvironment and found relatively sparse immune infiltration in ACC, which was consistent with previous reports[31]. ACC is traditionally characterized as an immune-depleted tumor, a condition believed to be influenced by adrenal glucocorticoid production[32]. It has been reported that CD4+ tumor-infiltrating lymphocytes negatively correlate with glucocorticoid levels in ACC patients[33]. In our study, CD4 +

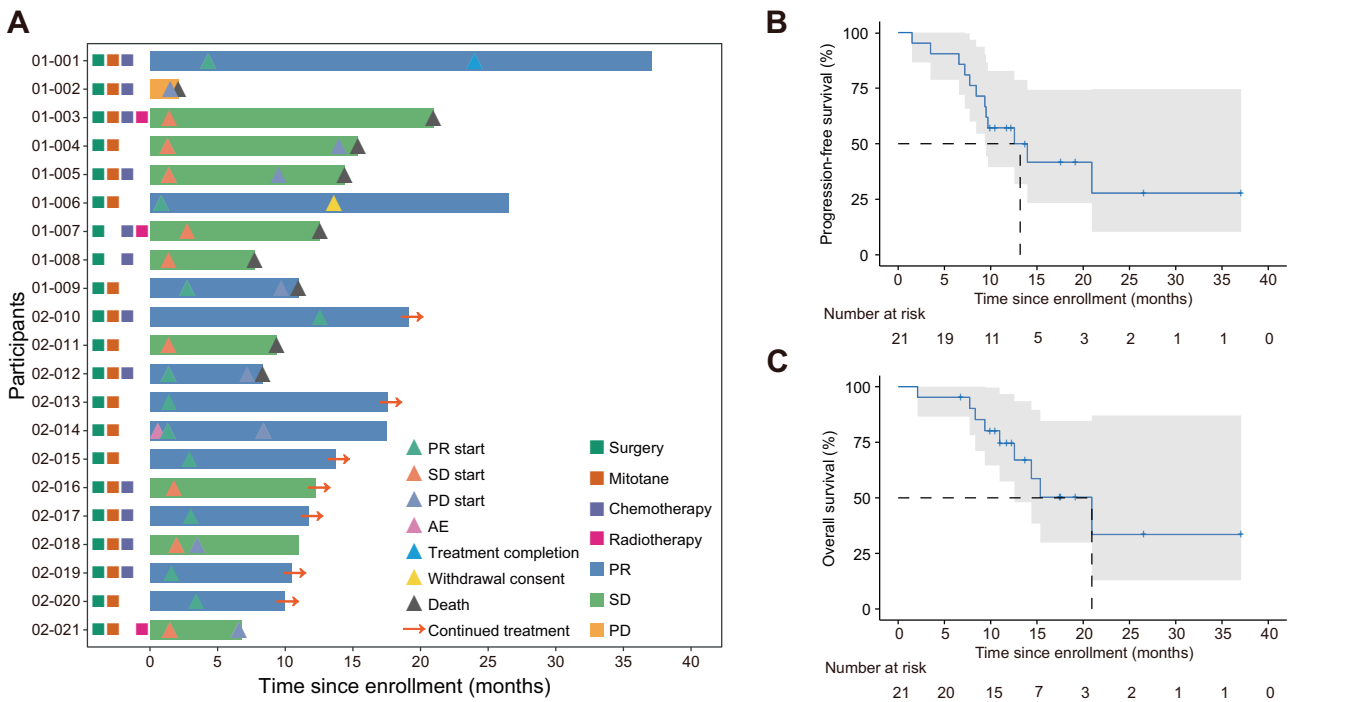

Fig. 3 | Clinical outcomes. A Swimmer plot for duration of follow-up in all patients ($n = 21$). Each bar represents one patient. **B** Kaplan-Meier curve of progression-free survival ($n = 21$). The shaded area represents the corresponding 95% confidence interval. **C** Kaplan-Meier curve of overall survival ($n = 21$). The shaded area represents the corresponding 95% confidence interval. PD progressive disease, PR partial response, SD stable disease, AE adverse event. Source data are provided as a Source Data file.

https://doi.org/10.1038/s41467-024-54661-9

Table 3 | Treatment related adverse events

	Overall (*N* = 21)							
TRAEs	**Grade 1**		**Grade 2**		**Grade 3**		**Grade 4**	
Fatigue	6	(28.6)	6	(28.6)	1	(4.8)	0	
Aspartate aminotransferase elevation	5	(23.8)	4	(19)	3	(14.3)	2	(9.5)
Alanine aminotransferase elevation	2	(9.5)	4	(19)	5	(23.8)	1	(4.8)
Hypertriglyceridemia	6	(28.6)	0		0		0	
Lymphopenia	0		5	(23.8)	4	(19)	1	(4.8)
Hypercholesterolemia	5	(23.8)	0		0		0	
Hypertension	3	(14.3)	2	(9.5)	0		0	
Reactive cutaneous capillary endothelial proliferation	4	(19)	0		0		0	
BNP elevation	4	(19)	0		0		0	
Leukocytopenia	2	(9.5)	2	(9.5)	0		0	
Nausea	2	(9.5)	2	(9.5)	0		0	
Hypothyroidism	2	(9.5)	2	(9.5)	0		0	
Anorexia	2	(9.5)	2	(9.5)	0		0	
Hypoalbuminema	3	(14.3)	0		0		0	
Hyponatremia	3	(14.3)	0		0		0	
Hypokalaemia	2	(9.5)	1	(4.8)	0		0	
Fever	2	(9.5)	1	(4.8)	0		0	
Anemia	2	(9.5)	0		1	(4.8)	0	
Vomiting	1	(4.8)	2	(9.5)	0		0	
Proteinuria	0		3	(14.3)	0		0	
Blood bilirubin elevation	2	(9.5)	0		0		0	
Hyperuricemia	2	(9.5)	0		0		0	
Hand-foot syndrome	2	(9.5)	0		0		0	
Constipation	1	(4.8)	1	(4.8)	0		0	
Neutropenia	1	(4.8)	1	(4.8)	0		0	
Diarrhea	0		2	(9.5)	0		0	
Oral mucositis	0		2	(9.5)	0		0	
Rash	0		2	(9.5)	0		0	
Anasarca	0		2	(9.5)	0		0	
Gastrointestinal bleeding	0		2	(9.5)	0		0	
Creatinine elevation	1	(4.8)	0		0		0	
Thrombocytopenia	1	(4.8)	0		0		0	
Pruritus	1	(4.8)	0		0		0	

Data are n (%). No grade 5 treatment-related adverse events were reported. Patients could report more than one adverse event. If a patient experienced multiple occurrences of the same adverse event, they were counted once at the maximum recorded grade.
TRAE treatment-related adverse event, *BNP* brain natriuretic peptide.

T cells, CD8 + T cells, and NK cells did not show a significant correlation with treatment response or with whether the tumor was hormonally functional. Given the confirmed variability in immune infiltration between primary and recurrent/metastatic tumors[33], and considering that the tissues analyzed in our study were predominantly from primary tumors previously surgically resected, it is crucial to further investigate whether the findings in the context of salvage therapy truly reflect the correlation between the immune microenvironment and the efficacy of combined treatment, as well as glucocorticoids.

We also reported the impact of circulating immune cells on the efficacy of the combined therapy in ACC. Patients who responded to camrelizumab plus apatinib had higher peripheral blood CD8 + T cell abundance prior to treatment. CD8+ T cells, also known as cytotoxic T lymphocytes, are well recognized for their anti-tumor functions[34]. Notably, naïve CD8 + T cells with higher CXCR3 expression likely played an important role in the treatment response. CXCR3+ naïve CD8 + T cells, considered young memory T cells, are more likely to differentiate and acquire effector functions, enabling timely immune responses against foreign antigens[35–37]. The CXCR3 axis is involved in the migration, differentiation, and activation of immune cells, contributing to tumor suppression[38]. CXCR3 expression in peripheral T cells has also been proposed as a predictor of immunotherapy efficacy, with enhanced CXCR3 signaling potentially aiding PD-1 inhibitors in suppressing tumor growth[39]. In addition, tumor response was associated with low pre-treatment circulating CD4 + T cell abundance. However, due to the limited sample size, we lack sufficient evidence to distinguish between different CD4 + T cell subtypes. Interestingly, we observed higher TIM-3 expression in CD4 + T cells in nonresponders. TIM-3 is a known co-inhibitory molecule that contributes to an immunosuppressive tumor environment[40]. Given the generally lower expression level of TIM-3 in CD4 + T cells, this finding requires further validation.

In addition, consistent with this study, a lower CD4 + /CD8 + T cell ratio was significantly associated with a superior objective response to anti-PD-1 immunotherapy in patients with gastric, esophageal, and colorectal cancers[41,42]. It has been reported that the proportions of CD4 + T cells and CD4 + /CD8 + T cell ratio significantly increased after immunotherapy in the peripheral blood of gastric cancer patients who responded to treatment[43]. In the present study, although changes in peripheral blood CD4+ or CD8 + T cells were not significant in ACC patients who responded to treatment, we observed a significant decrease in the CD4 + /CD8 + T cell ratio after treatment in patients who did not respond, largely attributed to a decrease in CD4 + T cells. Different CD4 + T cell subtypes may have opposing roles in tumor immunity; however, due to the lack of an analysis of CD4 + T cell subtypes after treatment, we cannot specify which subtypes of CD4 + T cells are declining. In addition, an analysis of tumor-infiltrating lymphocyte subtypes before and after treatment would also help to better explain the specific changes in lymphocyte subtypes in the peripheral blood.

Investigations into the impact of TCR diversity on the treatment response to immunotherapy have resulted in varied and sometimes conflicting findings. For instance, Postow et al. examined the effect of the initial TCR repertoire on melanoma patients undergoing immunotherapy and found that high TCR diversity in peripheral blood was associated with better survival outcomes[44]. Conversely, Hogan et al. reported that reduced TCR diversity predicted superior responses to PD-1 inhibitors and longer PFS[45]. In this study, we also observed that TCR diversity in peripheral blood was inversely correlated with tumor regression in ACC. Moreover, the presence of overlapping clones between the blood and tumor prior to immunotherapy provided more informative insights into clinical outcome. Specifically, a higher frequency of shared clones was associated with a more favorable treatment response[46]. Our findings confirmed this association, indicating that ACC patients with a higher overlap index were more likely to benefit from the combined therapy.

Exploring outcomes based on genomic characteristics and gut microbiome aimed to identify additional biomarkers of response. However, no significant association was found between the treatment response and TMB, somatic alterations, or microbial diversity.

As an early-phase exploratory trial, this study had several inherent limitations, including a small sample size and the lack of a control cohort. These factors may limit the ability to provide statistically meaningful information, particularly in the exploratory analysis of biomarkers. Meanwhile, the absence of post-treatment tumor tissue restricts the assessment of changes in the tumor microenvironment attributed to camrelizumab and apatinib treatment. Given the rarity of ACC, these constraints reflect the challenges of conducting clinical research in rare conditions. Furthermore, while mitotane has been shown to be safe when administered concurrently with immunotherapy[6,9], its role as a potent CYP3A4 inducer and its long

https://doi.org/10.1038/s41467-024-54661-9

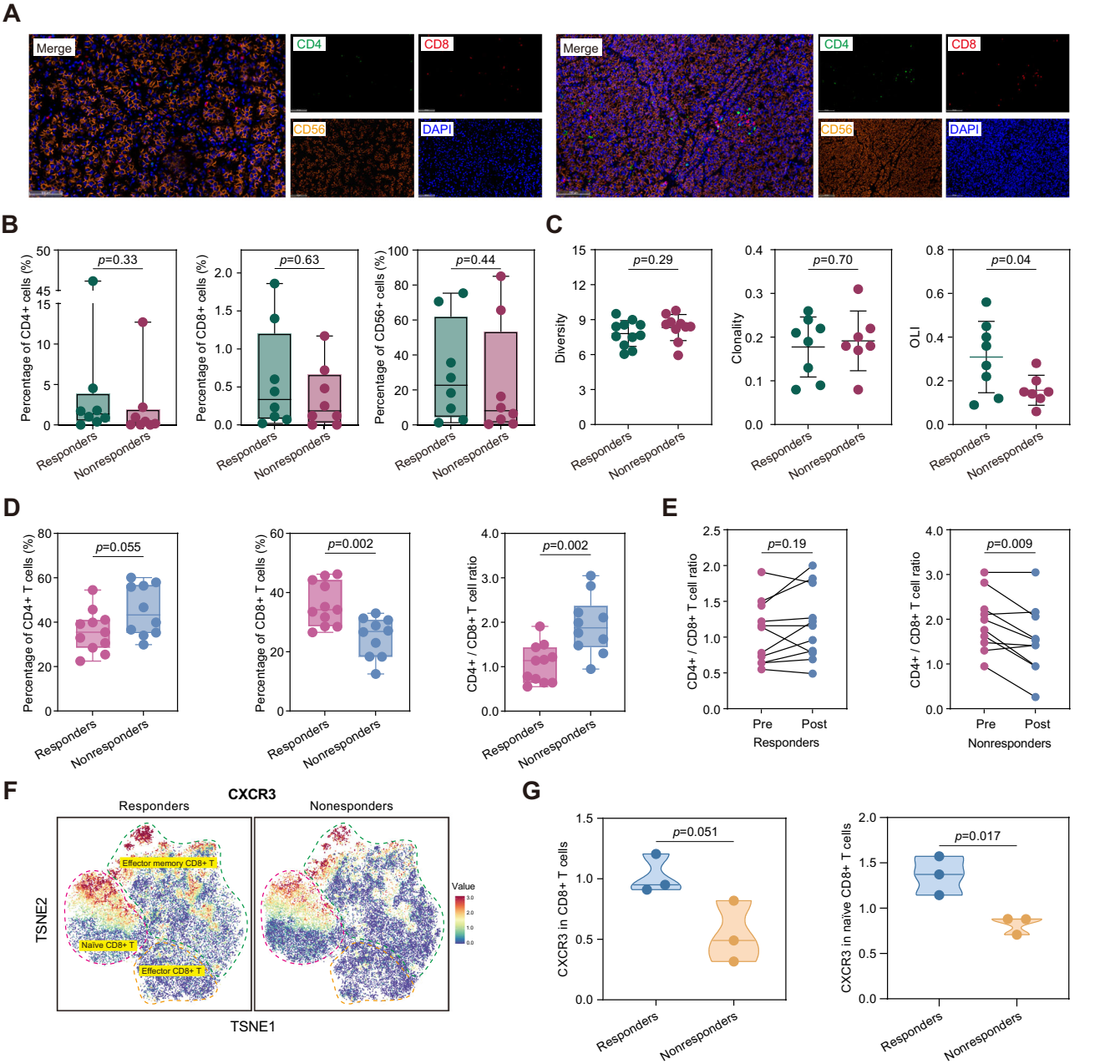

Fig. 4 | Tumor and systemic immune characteristics. A Representative immunofluorescence staining from one responder (left, Pt. 02-019) and one non-responder (right, Pt.02-016). Scale bar = 100 μm. **B** Comparisons of percentages of CD4 + , CD8 + , and CD56+ cells in pretreatment tumor tissues between responders ($n = 8$) and nonresponders ($n = 8$). Two-sided Mann–Whitney U test was used. Each dot represents an individual data point. Bounds of boxes represent the 25th and 75th percentiles, the center represents the median, and the whiskers represent the minimum and maximum values. **C** Comparisons of TCR diversity in peripheral blood (11 responders, 10 nonresponders), tumor tissue clonality (8 responders, 7 nonresponders), and overlap index (OLI) (8 responders, 7 nonresponders) between responders and nonresponders. Two-sided Student's *t* test was used. Each dot represents an individual data point, and bars represent the mean with standard deviation (SD). **D** Comparisons of immune cell subsets in pretreatment peripheral blood between responders ($n = 11$) and nonresponders ($n = 10$). Two-sided Student's *t* test was used. Each dot represents an individual data point. Bounds of boxes represent the 25th and 75th percentiles, the center represents the median, and the whiskers represent the minimum and maximum values. **E** Change in the CD4 + /CD8 + T cell ratio from pretreatment to after two treatment cycles in responders ($n = 11$) and nonresponders ($n = 10$). Two-sided paired samples *t* test was used. Each red dot represents an individual data point at baseline, while each blue dot represents an individual data point after two treatment cycles. The black line represents the direction of change in the CD4 + /CD8 + T cell ratio. **F** Heatmap of CXCR3 expression in CD8 + T cells (3 responders, 3 nonresponders). **G** Comparisons of CXCR3 expression levels in CD8 + T cells and naïve CD8 + T cells between responders ($n = 3$) and nonresponders ($n = 3$). Two-sided Student's *t* test was used. Each dot represents an individual data point. The center represents the median, and the truncation represents the minimum and maximum values. Source data are provided as a Source Data file.

half-life create pharmacokinetic interactions with other drugs, particularly TKIs[47,48]. In this study, although all patients who had previously received mitotane discontinued its use for at least four weeks before starting the study treatment, we did not monitor and record the mitotane blood level at enrollment and throughout the study period, which limits our ability to accurately assess its potential impact on the study medications.

In conclusion, the combination of camrelizumab and apatinib demonstrated promising activity and an acceptable safety profile in previously treated advanced ACC patients. Pre-treatment peripheral

https://doi.org/10.1038/s41467-024-54661-9

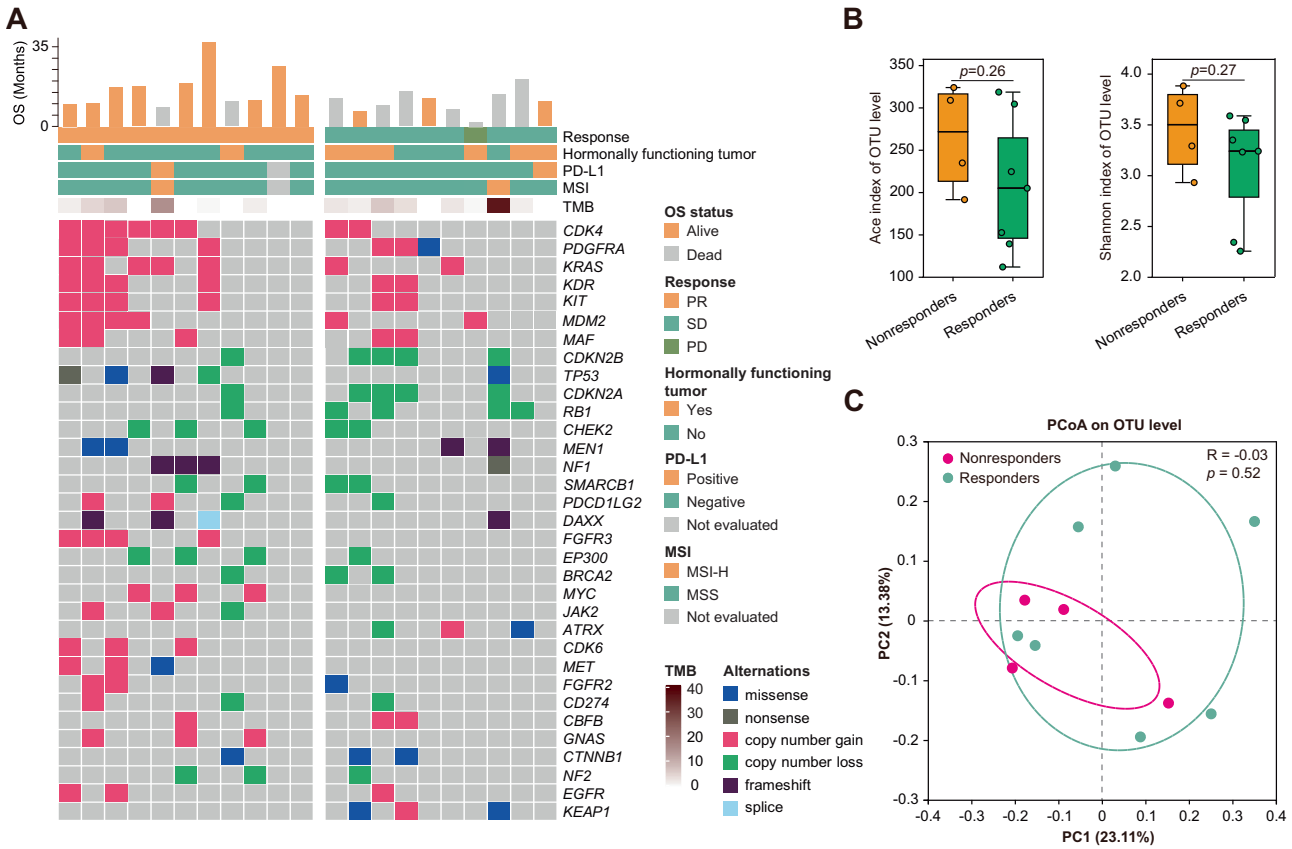

Fig. 5 | Genetic alteration and gut microbial diversity. A Oncoplot of mutated genes occurring in more than two patients ($n = 21$). **B** Alpha-diversity analysis of the gut microbiota at the OTU level, using ACE index and Shannon index (7 responders, 4 nonresponders). Two-sided Student's t test was used. Each dot represents an individual data point. Bounds of boxes represent the 25th and 75th percentiles, the center represents the median, and the whiskers represent the minimum and maximum values. **C** Beta-diversity analysis of the gut microbiota using principal coordinates analysis (PCoA) method based on unweighted-unifrac dissimilarity matrix (7 responders, 4 nonresponders). Each dot represents an individual data point, and the ellipse represents clustering of samples from responders or non-responders. Source data are provided as a Source Data file.

blood immune cell subsets may serve as potential predictors of treatment efficacy. Given these encouraging results, evaluation of camrelizumab in combination with apatinib in future research is warranted.

Methods

Study design and patients

This was an investigator-initiated, prospective, single-arm, open-label, phase 2 trial conducted at a single medical center, West China Hospital of Sichuan University. The study was approved and monitored by the Ethics Committee and the Clinical Trial Center of West China Hospital, Sichuan University. This study was conducted in accordance with the Declaration of Helsinki and the International Conference on Harmonization Good Clinical Practice guidelines. Written informed consent was obtained from all patients prior to study enrollment. This study was registered on ClinicalTrials.gov under the identifier NCT04318730, with the registration submitted on March 20, 2020.

Patients were eligible for inclusion if they were at least 18 years old; had a pathological diagnosis of recurrent or metastatic ACC; had failed one or more lines of therapy; had an ECOG performance status of 0 or 1; had at least one measurable lesion; and had adequate organ function. Key exclusion criteria included a history of treatment with immunotherapy, anti-angiogenic small molecule TKIs, or anti-angiogenic monoclonal antibodies; a history of uncontrolled hypertension; and an autoimmune condition requiring systemic therapy. The full study protocol is available in the Supplementary Information file. The first patient was enrolled on November 6, 2020, and the final patient was recruited on April 24, 2023.

Study treatment

All study patients received camrelizumab 200 mg intravenously on the first day of each 3-week cycle, combined with apatinib 250 mg orally once daily, until disease progression, intolerable toxicity, or withdrawal of consent. Dose modification of camrelizumab was not permitted. If adverse events occurred that were not alleviated by supportive care, dose adjustments and interruptions of apatinib were allowed. The initial dose reduction involved administering apatinib 250 mg once daily on a two days on, one day off schedule. Further reduction to 250 mg every other day was permitted if the adverse events persisted. Once the apatinib dose was reduced, it could not be escalated. If the adverse event did not improve to grade 1 or lower after the 4-week interruption, apatinib was permanently discontinued.

Study assessments

All patients underwent regular evaluations for response and safety. These included history and physical examination, adverse event assessment, hematological, biochemical, and endocrinological tests upon study entry and before each treatment cycle. Detailed endocrinological test information is provided in Supplementary Table 2. Baseline tumor response assessments were performed within 14 days before treatment using contrast-enhanced computed tomography or magnetic resonance imaging of the brain, chest, abdomen, pelvis, and

any other known sites of disease. Subsequent regular assessments were conducted every two cycles, following the same methodology as the baseline evaluations. Patients with clinically unstable disease could be evaluated at any time with unplanned imaging assessments.

The primary endpoint was the objective response rate (ORR), defined as the proportion of participants achieving a CR or PR per RECIST version 1.1. Both CR and PR had to be confirmed at least 4 weeks after the initial response. The best overall response was the best tumor response recorded at any point after treatment initiation. Secondary endpoints included PFS, defined as the time from the initiation of treatment to disease progression or death, whichever occurred first; OS, defined as the time from the treatment initiation to the date of death or the end of follow-up, whichever occurred first; and safety, defined as the incidence of TRAEs per NCI-CTCAE version 5.0.

Exploratory endpoints included molecular biomarker analyses and their association with treatment response. PD-L1 expression was assessed using the CPS with the PD-L1 22C3 pharmDx assay (concentration: 3 μg/mL; Dako, Agilent Technologies, Carpinteria, USA). Multiplex immunofluorescence was used to detect the percentages of CD4+ (clone 458G4A1, ready-to-use, Abcarta), CD8+ (clone 815R4B2, ready-to-use, Abcarta), and CD56+ (clone 682F4C5, ready-to-use, Abcarta) cells within the tumor-related area of pre-treatment tumor tissues.

TCR diversity in peripheral blood mononuclear cells (PBMCs) and clonality of tumor-infiltrating T cells in pre-treatment tissues were analyzed. Genomic DNA from PBMCs and tumor tissues was extracted using commercial kits (Qiagen, Duesseldorf, Germany) and sequenced for the variable CDR3 region of the TCR β-chain using the immunoSEQ assay, as previously described[49]. From the CDR3β data, T-cell diversity in PBMCs and clonality of tumor-infiltrating T cells were assessed. The overlap index (OLI) was calculated from the detection data of the TCR immunogroup bank, based on the number and abundance of shared clones between tumor-infiltrating T cells and circulating T cells.

The analysis of immune cell subsets was conducted on PBMCs obtained from pre-treatment blood samples using flow cytometry and mass cytometry (CyTOF) method with an immune-related panel consisting of 41 markers (Supplementary Table 3). Cells were initially stained with cisplatin to exclude dead cells, followed by staining with a cocktail of surface antibodies. After fixation with an intercalation solution (Maxpar Fix and Perm Buffer containing 250 nM 191/193Ir, Fluidigm), cells were stained with an intracellular antibody cocktail. The cells were then washed, resuspended, and mixed with 20% EQ beads before being acquired on a mass cytometer (Helios, Fluidigm). Data for each sample were debarcoded from raw data using a doublet-filtering scheme[50], normalized through bead normalization[51], and manually gated to exclude debris and dead cells using FlowJo software (FlowJo, Oregon, USA). The Phenograph algorithm was employed for clustering based on marker expression, with clusters annotated according to marker patterns[52]. The t-distributed stochastic neighbor embedding (t-SNE) dimension reduction technique was used to visualize the clusters and illustrate marker expression[53].

Tumor tissue samples, along with self-blood negative controls, were sequenced using a comprehensive 503 cancer-related panel. Genomic alterations and gene fusions/rearrangements, were identified using GATK, MuTect (version 1.1.4) (http://www.broadinstitute.org/cancer/cga/mutect), and BreakDancer[54], respectively. MSI status was assessed using MSIsensor (version 0.2)[55]. Tumors with an MSI score of 10 or higher were classified as MSI-H. TMB was calculated based on the number of all somatic nonsynonymous mutations, insertions, and deletions per megabase of coding regions sequenced.

Microbiota diversity of the gut prior to treatment was assessed using 16S rRNA sequencing. Data analysis of the gut microbiota was performed on the Majorbio Cloud platform (https://cloud.majorbio.com). Based on the OTUs information, α diversity indices, including ACE and Shannon indices, were calculated using Mothur v1.30.1[56]. The similarity among microbial communities in different samples was determined by principal coordinate analysis (PCoA) using the Vegan v2.5-3 package (https://vegandevs.github.io/vegan/).

Statistical analyses

A Simon's two-stage design was used to determine the sample size for the study[57,58]. Historical data indicated an ORR of 14% for single-agent pembrolizumab as salvage therapy in ACC[11]. To detect an approximate 26% improvement (reaching an ORR of 40%), with 80% power and a one-sided alpha of 0.05, a sample size of 19 patients was required. In stage I, nine patients were enrolled; if at least one of the nine patients exhibited a PR or CR, the study would proceed to stage II to enroll an additional 10 patients. The combination treatment would be considered worthwhile if six or more objective responses were observed among the 19 patients. Considering an anticipated 10% dropout rate, the study needed to enroll a total of 21 patients.

Analyses for all primary and secondary endpoints were conducted in the mITT population, including all patients who received at least one dose of the study drug. Continuous variables were presented as medians with interquartile range (IQR), while categorical variables were shown as frequency with corresponding percentage. The ORR was presented with its corresponding 95% CI, calculated using the Clopper-Pearson method. Median follow-up time was calculated using the reverse Kaplan-Meier method[59]. The median duration of response, median PFS, and median OS were estimated using the Kaplan-Meier method; corresponding 95% CIs were estimated using the Brookmeyer-Crowley method. Safety data was described using descriptive statistics.

Pearson's chi-square test or Fisher's exact test was used to assess the association of clinicopathological characteristics and genetic mutations with ORR. The normality of the distribution of continuous variables was confirmed using the Shapiro–Wilk normality test. If the data passed the normality test, Student's *t* test was used to examine the association of immune cell proportions in blood or tumor tissue, TCR diversity, or microbial diversity index with treatment response. If the distribution was not normal, the Mann–Whitney U test was applied. A paired student's *t* test was used to compare immune cell proportions before and after treatment. Pearson correlation coefficient was calculated to assess the correlations between the best tumor change and immune cell proportion or TCR diversity. Statistical analysis was performed using GraphPad Prism software (version 9.4.1, San Diego, California) and R software (version 3.6.1, Vienna, Austria).

Reporting summary

Further information on research design is available in the Nature Portfolio Reporting Summary linked to this article.

Data availability

All raw sequencing data generated in this study have been deposited in the National Genomics Data Center (NGDC) under the accession code HRA008803, HRA008789, and HRA008669. The raw sequencing data contain information unique to individuals and are available under controlled access. Access to the data can be requested by completing the application form via GSA-Human System and is granted by the corresponding Data Access Committee. Additional guidance can be found at the GSA-Human System website [https://ngdc.cncb.ac.cn/gsa-human/document/GSA-Human_Request_Guide_for_Users_us.pdf]. The raw patient data are protected and not publicly available due to data privacy laws. The de-identified individual patient data will be available upon reasonable request for academic research purposes by contacting the corresponding author (pxx2014@163.com) for 10 years. The study protocol is available in the Supplementary Information file. The remaining data are available within the Article, Supplementary Information, and Source Data file. Source data are provided with this paper.

References

1. Else, T. et al. Adrenocortical carcinoma. *Endocr. Rev.* **35**, 282–326 (2014).
2. Fassnacht, M. et al. Adrenocortical carcinomas and malignant phaeochromocytomas: ESMO-EURACAN clinical practice guidelines for diagnosis, treatment and follow-up. *Ann. Oncol.* **31**, 1476–1490 (2020).
3. Megerle, F. et al. Mitotane monotherapy in patients with advanced adrenocortical carcinoma. *J. Clin. Endocrinol. Metab.* **103**, 1686–1695 (2018).
4. Reidy-Lagunes, D. L. et al. Complete responses to mitotane in metastatic adrenocortical carcinoma-a new look at an old drug. *Oncologist* **22**, 1102–1106 (2017).
5. Fassnacht, M. et al. Combination chemotherapy in advanced adrenocortical carcinoma. *N. Engl. J. Med.* **366**, 2189–2197 (2012).
6. Le Tourneau, C. et al. Avelumab in patients with previously treated metastatic adrenocortical carcinoma: Phase 1b results from the JAVELIN solid tumor trial. *J. Immunother. Cancer* **6**, 111 (2018).
7. Raj, N. et al. PD-1 blockade in advanced adrenocortical carcinoma. *J. Clin. Oncol.* **38**, 71–80 (2020).
8. Klein, O. et al. Combination immunotherapy with ipilimumab and nivolumab in patients with advanced adrenocortical carcinoma: a subgroup analysis of CA209-538. *Oncoimmunology* **10**, 1908771 (2021).
9. Remde, H. et al. Outcome of immunotherapy in adrenocortical carcinoma: a retrospective cohort study. *Eur. J. Endocrinol.* **188**, 485–493 (2023).
10. Carneiro, B. A. et al. Nivolumab in metastatic adrenocortical carcinoma: Results of a phase 2 trial. *J. Clin. Endocrinol. Metab.* **104**, 6193–6200 (2019).
11. Habra, M. A. et al. Phase II clinical trial of pembrolizumab efficacy and safety in advanced adrenocortical carcinoma. *J. Immunother. Cancer* **7**, 253 (2019).
12. Connell, C. M. et al. Cancer immunotherapy trials underutilize immune response monitoring. *Oncologist* **23**, 116–117 (2018).
13. Kroiss, M. et al. Sunitinib inhibits cell proliferation and alters steroidogenesis by down-regulation of HSD3B2 in adrenocortical carcinoma cells. *Front Endocrinol* (*Lausanne*) 2, 27 (2011).
14. Kroiss, M. et al. Sunitinib in refractory adrenocortical carcinoma: a phase II, single-arm, open-label trial. *J. Clin. Endocrinol. Metab.* **97**, 3495–3503 (2012).
15. Yi, M. et al. Synergistic effect of immune checkpoint blockade and anti-angiogenesis in cancer treatment. *Mol. Cancer* **18**, 60 (2019).
16. Ding, X. et al. Camrelizumab plus apatinib in patients with recurrent or metastatic nasopharyngeal carcinoma: An open-label, single-arm, phase II study. *J. Clin. Oncol.* **41**, 2571–2582 (2023).
17. Meng, X. et al. Camrelizumab plus apatinib as second-line treatment for advanced oesophageal squamous cell carcinoma (CAP 02): a single-arm, open-label, phase 2 trial. *Lancet Gastroenterol. Hepatol.* **7**, 245–253 (2022).
18. Xu, J. et al. Camrelizumab in combination with apatinib in patients with advanced hepatocellular carcinoma (RESCUE): A nonrandomized, open-label, phase II trial. *Clin. Cancer Res* **27**, 1003–1011 (2021).
19. Cheng, H. et al. Camrelizumab plus apatinib in patients with high-risk chemorefractory or relapsed gestational trophoblastic neoplasia (CAP 01): A single-arm, open-label, phase 2 trial. *Lancet Oncol.* **22**, 1609–1617 (2021).
20. Lan, C. et al. Camrelizumab plus apatinib in patients with advanced cervical cancer (CLAP): A multicenter, open-label, single-arm, phase II trial. *J. Clin. Oncol.* **38**, 4095–4106 (2020).
21. Bedrose, S. et al. Combined lenvatinib and pembrolizumab as salvage therapy in advanced adrenal cortical carcinoma. *J. Immunother. Cancer* **8**, https://doi.org/10.1136/jitc-2020-001009 (2020).
22. Lee, W. S., Yang, H., Chon, H. J. & Kim, C. Combination of anti-angiogenic therapy and immune checkpoint blockade normalizes vascular-immune crosstalk to potentiate cancer immunity. *Exp. Mol. Med.* **52**, 1475–1485 (2020).
23. Zhou, C. et al. Efficacy and biomarker analysis of camrelizumab in combination with apatinib in patients with advanced nonsquamous NSCLC previously treated with chemotherapy. *Clin. Cancer Res.* **27**, 1296–1304 (2021).
24. Liu, J. et al. Efficacy and safety of camrelizumab combined with apatinib in advanced triple-negative breast cancer: an open-label phase II trial. *J. Immunother. Cancer* **8**, https://doi.org/10.1136/jitc-2020-000696 (2020).
25. Pegna, G. J. et al. The immunotherapy landscape in adrenocortical cancer. *Cancers (Basel)* **13**, https://doi.org/10.3390/cancers13112660 (2021).
26. Fan, Y. et al. Camrelizumab plus apatinib in extensive-stage SCLC (PASSION): A multicenter, two-stage, phase 2 trial. *J. Thorac. Oncol.* **16**, 299–309 (2021).
27. Maher, V. E. et al. Analysis of the association between adverse events and outcome in patients receiving a programmed death protein 1 or programmed death ligand 1 antibody. *J. Clin. Oncol.* **37**, 2730–2737 (2019).
28. Fay, A. P. et al. Programmed death ligand-1 expression in adrenocortical carcinoma: an exploratory biomarker study. *J. Immunother. Cancer* **3**, 3 (2015).
29. Paijens, S. T., Vledder, A., de Bruyn, M. & Nijman, H. W. Tumor-infiltrating lymphocytes in the immunotherapy era. *Cell Mol. Immunol.* **18**, 842–859 (2021).
30. Hiam-Galvez, K. J., Allen, B. M. & Spitzer, M. H. Systemic immunity in cancer. *Nat. Rev. Cancer* **21**, 345–359 (2021).
31. Wu, K. et al. Discovery of a glucocorticoid receptor (GR) activity signature correlates with immune cell infiltration in adrenocortical carcinoma. *J. Immunother. Cancer* **11**, https://doi.org/10.1136/jitc-2023-007528 (2023).
32. Georgantzoglou, N., Kokkali, S., Tsourouflis, G. & Theocharis, S. Tumor microenvironment in adrenocortical carcinoma: Barrier to immunotherapy success? *Cancers (Basel)* **13**, https://doi.org/10.3390/cancers13081798 (2021).
33. Landwehr, L. S. et al. Interplay between glucocorticoids and tumor-infiltrating lymphocytes on the prognosis of adrenocortical carcinoma. *J. Immunother. Cancer* **8**, https://doi.org/10.1136/jitc-2019-000469 (2020).
34. Hamann, D. et al. Phenotypic and functional separation of memory and effector human CD8+ T cells. *J. Exp. Med.* **186**, 1407–1418 (1997).
35. De Simone, G. et al. CXCR3 identifies human naive CD8(+) T cells with enhanced effector differentiation potential. *J. Immunol.* **203**, 3179–3189 (2019).
36. Murata, K. et al. Identification of a novel human memory T-cell population with the characteristics of stem-like chemo-resistance. *Oncoimmunology* **5**, e1165376 (2016).
37. Fulton, R. B. et al. The TCR's sensitivity to self peptide-MHC dictates the ability of naive CD8(+) T cells to respond to foreign antigens. *Nat. Immunol.* **16**, 107–117 (2015).
38. Tokunaga, R. et al. CXCL9, CXCL10, CXCL11/CXCR3 axis for immune activation - A target for novel cancer therapy. *Cancer Treat. Rev.* **63**, 40–47 (2018).
39. Han, X. et al. Role of CXCR3 signaling in response to anti-PD-1 therapy. *EBioMedicine* **48**, 169–177 (2019).
40. Tang, R., Rangachari, M. & Kuchroo, V. K. Tim-3: A co-receptor with diverse roles in T cell exhaustion and tolerance. *Semin Immunol.* **42**, 101302 (2019).
41. Xu, S. et al. Association of the CD4(+)/CD8(+) ratio with response to PD-1 inhibitor-based combination therapy and dermatological toxicities in patients with advanced gastric and esophageal cancer. *Int. Immunopharmacol.* **123**, 110642 (2023).

42. Cheng, Y. K. et al. Association of peripheral blood biomarkers with response to anti-PD-1 immunotherapy for patients with deficient mismatch repair metastatic colorectal cancer: A multicenter cohort study. *Front Immunol.* **13**, 809971 (2022).
43. Wang, X., Liu, X., Dai, H. & Jia, J. Association of lymphocyte subsets with the efficacy and prognosis of PD-1 inhibitor therapy in advanced gastric cancer: Results from a monocentric retrospective study. *BMC Gastroenterol.* **24**, 113 (2024).
44. Postow, M. A. et al. Peripheral T cell receptor diversity is associated with clinical outcomes following ipilimumab treatment in metastatic melanoma. *J. Immunother. Cancer* **3**, 23 (2015).
45. Hogan, S. A. et al. Peripheral blood TCR repertoire profiling may facilitate patient stratification for immunotherapy against melanoma. *Cancer Immunol. Res.* **7**, 77–85 (2019).
46. Porciello, N., Franzese, O., D'Ambrosio, L., Palermo, B. & Nistico, P. T-cell repertoire diversity: friend or foe for protective antitumor response? *J. Exp. Clin. Cancer Res* **41**, 356 (2022).
47. Altieri, B. et al. Recovery of adrenal function after stopping mitotane in patients with adrenocortical carcinoma. *Eur. J. Endocrinol.* **190**, 139–150 (2024).
48. Kroiss, M., Quinkler, M., Lutz, W. K., Allolio, B. & Fassnacht, M. Drug interactions with mitotane by induction of CYP3A4 metabolism in the clinical management of adrenocortical carcinoma. *Clin. Endocrinol. (Oxf.)* **75**, 585–591 (2011).
49. Robins, H. S. et al. Comprehensive assessment of T-cell receptor beta-chain diversity in alphabeta T cells. *Blood* **114**, 4099–4107 (2009).
50. Zunder, E. R. et al. Palladium-based mass tag cell barcoding with a doublet-filtering scheme and single-cell deconvolution algorithm. *Nat. Protoc.* **10**, 316–333 (2015).
51. Finck, R. et al. Normalization of mass cytometry data with bead standards. *Cytom. A* **83**, 483–494 (2013).
52. Levine, J. H. et al. Data-driven phenotypic dissection of AML reveals progenitor-like cells that correlate with prognosis. *Cell* **162**, 184–197 (2015).
53. Jamieson, A. R. et al. Exploring nonlinear feature space dimension reduction and data representation in breast Cadx with Laplacian eigenmaps and t-SNE. *Med Phys.* **37**, 339–351 (2010).
54. Chen, K. et al. BreakDancer: An algorithm for high-resolution mapping of genomic structural variation. *Nat. Methods* **6**, 677–681 (2009).
55. Niu, B. et al. MSIsensor: Microsatellite instability detection using paired tumor-normal sequence data. *Bioinformatics* **30**, 1015–1016 (2014).
56. Schloss, P. D. et al. Introducing mothur: Open-source, platform-independent, community-supported software for describing and comparing microbial communities. *Appl Environ. Microbiol.* **75**, 7537–7541 (2009).
57. Simon, R. Optimal two-stage designs for phase II clinical trials. *Control Clin. Trials* **10**, 1–10 (1989).
58. Jung, S. H., Lee, T., Kim, K. & George, S. L. Admissible two-stage designs for phase II cancer clinical trials. *Stat. Med.* **23**, 561–569 (2004).
59. Schemper, M. & Smith, T. L. A note on quantifying follow-up in studies of failure time. *Control Clin. Trials* **17**, 343–346 (1996).

Acknowledgements

This work was supported by the National Key Research and Development Program of China (2021YFE0206600, X.P.), the Clinical Research Incubation Project of West China Hospital (2020HXFH031, 20HXFH037, X.P.), the Sichuan Science and Technology Program (2022YFSY0012, 2021ZYCD011, 2021YFSY0008, 2021CDDZ-25, 2021CDZG-24, X.P.), the Chengdu International Science and Technology Cooperation Program (2022-GH03-00004-HZ, X.P.), the West China Nursing Discipline Development Special Fund Project (HXHL21008, X.P.), the Post-Doctor Research Project, West China Hospital, Sichuan University (2020HXBH119, X.P.), the Translational Medicine Fund of West China Hospital (CGZH19002, X.P.), and the China Medical Board (Grant #22-482, X.P.). The funders had no role in study design, data collection and analysis, decision to publish, or preparation of the manuscript. We sincerely thank the patients and their families for their participation in this study. We also extend our gratitude to the study coordinators and nurses for their dedication and enthusiasm. We appreciate the support from Jiangsu Hengrui Pharmaceuticals. We also thank Zhejiang Puluoting Health Technology Co., Ltd. for their work in performing CyTOF. Additionally, we thank Yan Wang, Jian Yang, Xiang-Yi Ren, Cong Li, and Jing-Yao Zhang from the Core Facilities, West China Hospital of Sichuan University for their assistance with sample processing.

Author contributions

Conception and design: Xing-Chen Peng, Yu-Chun Zhu, Qiang Wei, Ji-Yan Liu, Zhi-Gong Wei, Jing-Jing Wang, Zhe-Ran Liu, Yi-Yan Pei, Yu Min, Rui-Dan Li, Li Yang Provision of study materials or patients: Xing-Chen Peng, Yu-Chun Zhu, Qiang Wei, Ji-Yan Liu Collection and assembly of data: Yu-Chun Zhu, Zhi-Gong Wei, Jing-Jing Wang, Dong Li, Zhi-Hui Li, Zhe-Ran Liu, Yi-Yan Pei, Jin Jing, Yu Min, Rui-Dan Li, Li Yang Data analysis and interpretation: Yu-Chun Zhu, Zhi-Gong Wei, Jing-Jing Wang, Xing-Chen Peng. Manuscript writing: All authors. Final approval of manuscript: All authors. Accountable for all aspects of the work: All authors.

Competing interests

The authors declare no competing interests.

Additional information

Supplementary information The online version contains supplementary material available at https://doi.org/10.1038/s41467-024-54661-9.

Correspondence and requests for materials should be addressed to Xing-Chen Peng.

Peer review information *Nature Communications* thanks Barbara Altieri, Sara Bedrose, Martin Fassnacht and the other, anonymous, reviewer(s) for their contribution to the peer review of this work. A peer review file is available.